Master 1 Internship

Low frequency waves in dual temeprature plasma mediums

Master Sciences de l'Océan, de l'Atmosphère et du Climat

Clement LY, under the supervision of Dr. D. Graham and Pr. P. Rairoux

Contents

1 Acknowledgements

I would like to express my deepest gratitude to Pr. Daniel Graham, for their guidance, and encouragement all throughout my internship. I am also profoundly thankful to Dr. Alain Miffre and Pr. Patrick Rairoux for their careful help both during and before this ordeal, and whose expertise and dedication have greatly enriched my understanding of physics.

I would like to extend my sincere appreciation to Pr. Yuri Khotyaintsev and all the staff at IRF Uppsala, as wekk for their assistance and hospitality during my internship, as well as the administrative staff of Uppsala University for making this internship possible. Same regards extend to all the staff of University of Lyon, specially to Flavian Bouchet, for their help on organizing my first international academic trip.

Finally, for her unwavering support, her care and her trust, I'll thank humbly my mother.

2 Introduction

It is hard to study plasma physics without encountering the effects of Electromagnetic Ion Cyclotron waves. Solely on the planetary scale, they represent one of the key of wave-particle interaction in the ionosphere, due to their role on loss processes of highly energetic electrons [1]. Ranging from 0.1 to 10Hz, they are often linked to strong auroral effects [2], local and global magnetic structure changes [3], as well as direct injection [4].

The generation of this waves is caused, in magnetospheric conditions, by a sharp anisotropy of temperature [5]. Those waves are left hand polarized and we mostly observe them in parallel propagation in regards to the magnetic field. A mixed medium, incorporating heavier ions, can induce oblique propagation at the cost of a strong dampening.

In order to best represent this behaviors, we here study a MHD model including different fluid temeperatures and compare it to an event exhibiting strong low frequency waves.

3 Theoretical background

When studying electromagnetic waves in low-frequency plasma, we chose a thermal fluid model because of its ability to capture the essential physics of wave-plasma interactions in this regime. At low frequencies, electromagnetic waves have long wavelengths, resulting in slowly oscillating electric and magnetic fields, well above Debye scales. Charged particles in the plasma, respond to these slow variations by moving collectively, exhibiting fluid-like behavior. This makes the fluid approximation particularly suitable, as it focuses on the macroscopic motion of the plasma rather than the kinetic details of individual particles.

In this context, the thermal-fluid plasma model simplifies the problem by focusing on bulk quantities such as plasma density, velocity, and temperature, which are essential for understanding the plasma response to low-frequency electromagnetic fields. Unlike kinetic models, which track the dynamics of individual particles, the fluid approach is more effective in capturing the overall plasma behavior at these frequencies, and lightening significantly the calculations.

In addition, thermal effects, such as pressure and temperature gradients, play an important role in influencing plasma dynamics at low frequencies. The thermal fluid model incorporates these effects through energy equations, providing a more accurate representation of key phenomena such as heat conduction and energy exchange between particles. These processes are often essential for understanding wave propagation, damping, and plasma stability under low-frequency oscillations.

This model also aligns with the principles of magneto hydrodynamics (MHD), a framework that describes the behavior of magnetized fluids. MHD theory is particularly relevant for the study of low-frequency waves such as Alfvén waves or magnetosonic waves, where both fluid dynamics and magnetic effects are central. The thermal fluid model, by including temperature and pressure effects, extends the MHD approach, making it well suited to the analysis of complex interactions between electromagnetic waves and plasma in real-world scenarios.

Of course, the elementary equations hence are the Lorentz Equation:

$$\frac{d\vec{p}}{dt} = m.\frac{d\vec{v}}{dt} = q.(\vec{E} + \vec{v} \times \vec{B}) \tag{1}$$

As well as the Maxwell equations:

$$\vec{\nabla}.\vec{E} = \frac{\rho}{\epsilon_0} = \frac{e(n_i - n_e)}{\epsilon_0} \tag{2}$$

$$\vec{\nabla}.\vec{B} = 0 \tag{3}$$

$$\vec{\nabla} \times \vec{E} = -\frac{\partial \vec{B}}{\partial t} \tag{4}$$

$$\vec{\nabla} \times \vec{B} = \mu_0 \vec{j} + \epsilon_0 \mu_0 \frac{\partial \vec{E}}{\partial t} \tag{5}$$

Combining 1 with the Navier Stokes equations, we obtain a set of equations such as :

$$\frac{\partial n_j}{\partial t} + \nabla.(n_j V_j) = 0 \tag{6}$$

$$m_j n_j \left(\frac{\partial V_j}{\partial t} + (V_j.\nabla)V_j \right) = \epsilon_j e n_j (E + V_j \times B) - \nabla P_j \tag{7}$$

$$P_j = P_{0,j} \left(\frac{n_j}{n_{o,j}} \right)^{\gamma_j} \tag{8}$$

This highly nonlinear equation isn't very exploitable, as such we can consider a perturbation for any quantity Q such as :

$$Q = Q_0 + \delta Q \tag{9}$$

Without narrowing of cases, we consider $\vec{B_0} = (0, 0, B_0)$. Exploring only the first harmonic solutions, we obtain :

$$\delta Q(\omega, k) = \delta Q exp(-i\omega t + ik_x x + ik_z z) \tag{10}$$

Using maxwell euqatios, this leads to :

$$n \times n \times \delta E + K.\delta E = 0 \tag{11}$$

Taking into account the mass conservation equation, we obtain :

$$\delta n_j = \frac{n_j}{\omega}(k_x \delta V_{x,j} + k_z \delta V_{z,j}) \tag{12}$$

Then, by linearizing the mass conservation equations for each species, as found in [6],we can obtain finally :

$$\delta V_{x,j} = \frac{e}{m_j D_j}(i\epsilon_j\omega(\omega^2 - \gamma_j v_j^2 k_z^2)\delta E_x - \Omega_{cj}(\omega^2 - \gamma_j v_j^2 k_z^2)\delta E_y + i\epsilon_j\omega\gamma_j v_j^2 k_x k_z \delta E_z) \quad (13)$$

$$\delta V_{y,j} = \frac{e}{m_j D_j}(\Omega_{cj}(\omega^2 - \gamma_j v_j^2 k_z^2)\delta E_x + i\epsilon_j\omega(\omega^2 - \gamma_j v_j^2 k^2)\delta E_y + \Omega_{cj}\gamma_j v_j^2 k_x k_z \delta E_z) \quad (14)$$

$$\delta V_{z,j} = \frac{e}{m_j D_j}(i\epsilon_j\omega\gamma_j v_j^2 k_x k_z \delta E_x - \Omega_{cj}\gamma_j v_j^2 k_x k_z \delta E_y + i\epsilon_j\omega(\omega^2 - \Omega_{cj}^2 - \gamma_j v_j^2 k_x^2)\delta E_z) \quad (15)$$

With :

$$D_j = \omega^2(\omega^2 - \gamma_j \nu_j^2 k^2) - \Omega_{cj}^2(\omega^2 - \gamma_j \nu_j^2 k_z^2) \quad (16)$$

The dispersion relationship of the wave hence becomes, using 11:

$$\begin{pmatrix} K_{xx} - n_z^2 & K_{xy} & K_{xz} + n_x n_z \\ -K_{xy} & K_{yy} - n^2 & K_{yz} \\ K_{xz} + n_x n_z & -K_{yz} & K_{zz} - n_x^2 \end{pmatrix} \begin{pmatrix} \delta E_x \\ \delta E_y \\ \delta E_z \end{pmatrix} = 0 \quad (17)$$

With:

$$K_{xx} = 1 - \sum_j \frac{\omega_{pj}^2(\omega^2 - \gamma_j \nu_j^2 k_z^2)}{D_j} \quad (18)$$

$$K_{xy} = -\sum_j i\epsilon_j \frac{\omega_{pj}^2 \Omega_{cj}(\omega^2 - \gamma_j \nu_j^2 k_z^2)}{\omega D_j} \quad (19)$$

$$K_{xz} = -\sum_j \frac{\omega_{pj}^2 \gamma_j \nu_j^2 k_z k_z)}{D_j} \quad (20)$$

$$K_{yy} = 1 - \sum_j \frac{\omega_{pj}^2(\omega^2 - \gamma_j \nu_j^2 k^2)}{D_j} \quad (21)$$

$$K_{yz} = \sum_j i\epsilon_j \frac{\Omega_{cj}\omega_{pj}^2 \gamma_j \nu_j^2 k^2}{D_j} \quad (22)$$

$$K_{zz} = 1 - \sum_j \frac{\omega_{pj}^2(\omega^2 - \Omega_{cj}^2 - \gamma_j \nu_j^2 k_x^2)}{D_j} \quad (23)$$

The solvabitlity of the system is conditioned by the nullity of it's determinant :

$$\begin{gathered} \left(K_{xx}^2 - n_z^2\right)\left[\left(K_{yy} - n^2\right)\left(K_{zz} - n_x^2\right)\right. \\ +K_{yz}^2 + K_{xy}\left[K_{xy}\left(K_{zz} - n_x^2\right)\right. \\ \left.+K_{yz}\left(K_{xz} + n_x n_z\right)\right] + \left(K_{xz} + n_x n_z\right) \\ \left[K_{xy}K_{yz} - \left(K_{yy} - n^2\right)\left(K_{xz} + n_x n_z\right)\right] = 0. \end{gathered} \quad (24)$$

In order to solve this system, we use matlab native solving method in order to obtain the solution map, the trust region dogleg algorithm, as dispersion relations can pose significant challenges due to their nonlinear nature and the potential for multiple singularities.

The combination of the use of the trust region framework, which limits steps to a bounded region to maintain stability, and the dogleg method, which optimally combines steepest descent and Newtonian steps for efficient convergence. This dual approach makes the algorithm particularly suited to navigate the complex solution landscapes typical of dispersion relations. One of the main challenges have been to optimize those two parameters in order to maintain efficiency while creating a minimal amount of artificial singularities [7].

In this problem where the dispersion relation is ill-conditioned, with abrupt transitions, the trust region dogleg algorithm offers great robustness compared to others heavier methods, offering a balance between fast initial convergence via gradient descent and fast final convergence via Newton's method.

4 Results

In order to observe the first effects of the change in composition, we first observe the Alfven propagation, lowest frequency of our model. We've chosen, in the case of mixed phases, plasmic values similar to the first event described later in part 5, with however a strong 50-50 share between hot and cold ions. Alfven propagation is usually limited to parallel propagation with transverse perturbation of the electric field. Here, we can consider that an hybridation is observed with magnetosonic modes allows it to travel obliquely.

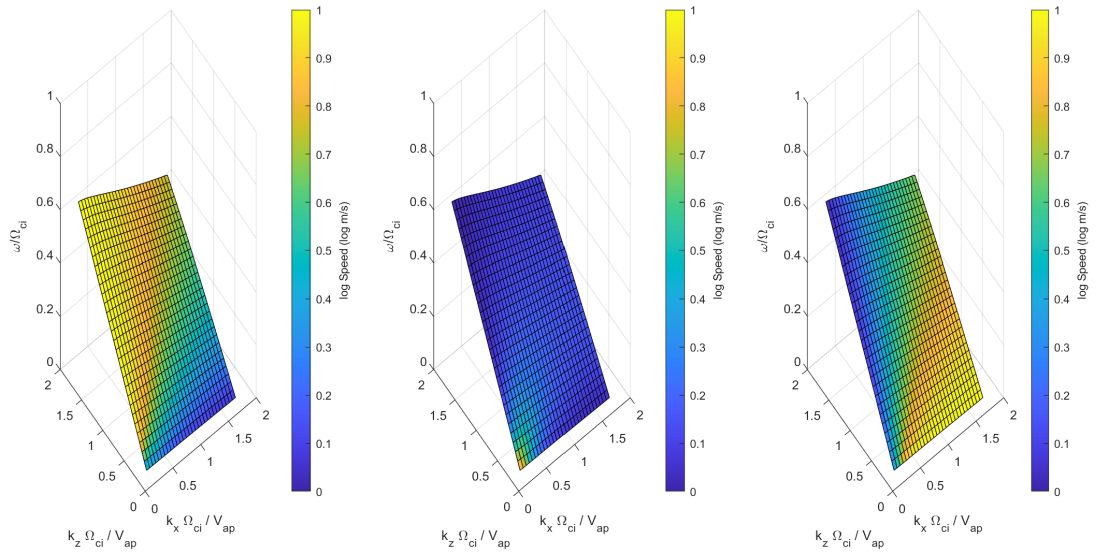

Figure 1: Relative strength of the X, Y and Z component, from left to right, of the electric field perturbation for a single protonic phase

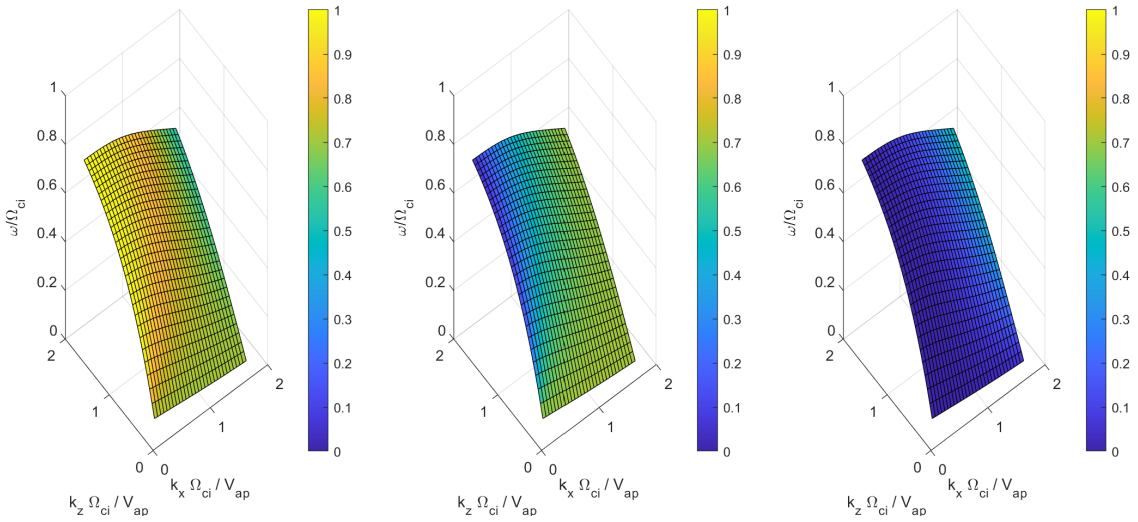

Figure 2: Relative strength of the X, Y and Z component, from left to right, of the electric field perturbation for a hot and a cold protonic phases

In Fig.1 and Fig.2, we observe the different share that each direction of the electric field. We can observe a change in the phase speed value (defined as the local derivative of frequency in a given direction of propagation), most notably at higher wave numbers.

Moreover, it is visible that under conditions of higher oblique propagation, the electric field generates points at weaker magnetosonic perturbations in a mixed-phase plasma compared to a simple-phase plasma. This disparity is primarily due to the

presence of hot ions in the mixed phase. These hot ions possess considerably higher thermal velocities and stronger inertia, making it much more difficult for the electric field to displace them from their natural gyration around the magnetic field lines, in contrast to their cooler counterparts in a simple-phase plasma. The increased inertia of the hot ions effectively resists the perturbations, reducing the overall efficiency of energy transfer from the electric field to the magnetosonic waves. As a result, the protons in the mixed-phase plasma are harder to push out of their guiding-center motion, leading to enhanced wave-particle interactions that manifest as strong damping of the magnetosonic waves.

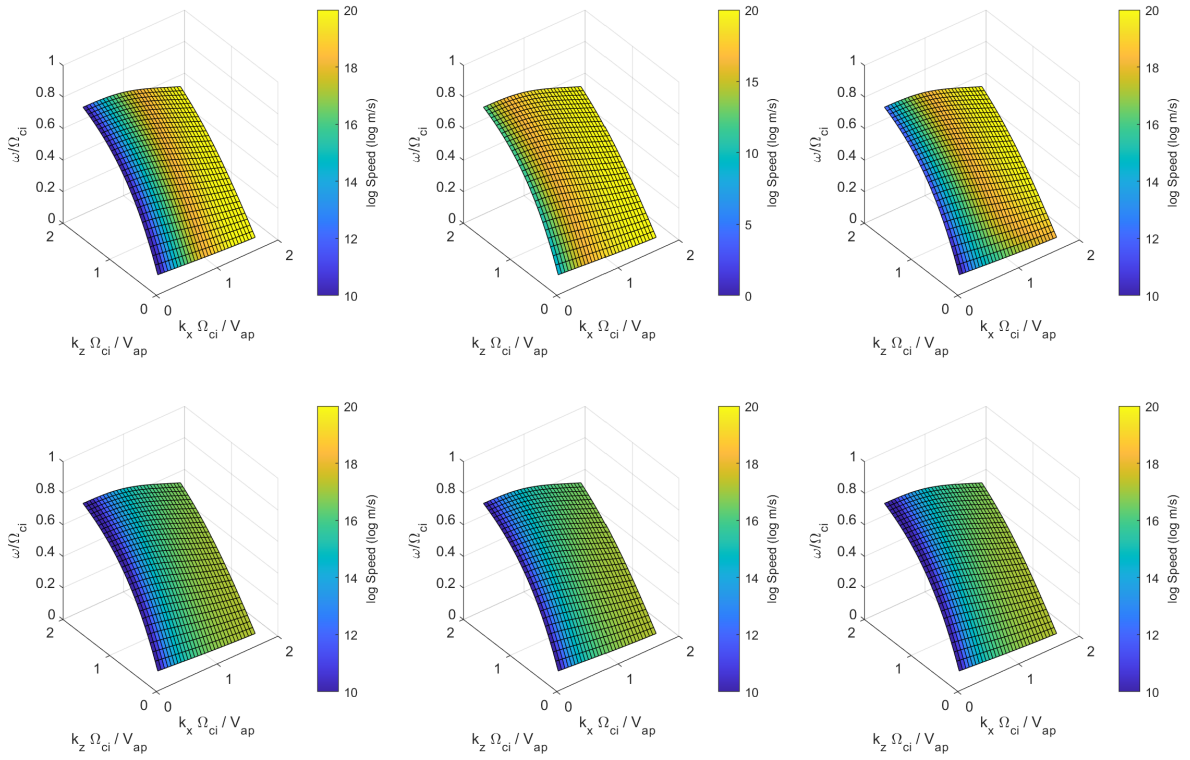

Figure 3: Speed of protons in a hot cold mix. Top row is the hot protons speeds, bottom row is the cold protons, in direction X, Y, Z from left to right

We also observe that the velocity distribution among protons is unevenly shared, even in cases where the plasma contains an equal number of hot and cold protons. The hot protons, because of their higher thermal energy, exhibit greater mobility compared to their cooler counterparts.

We can note that changes in the parallel wave number result in minimal variations in the overall ion speed. This suggests that the speed of wave propagation is relatively insensitive to variations in the parallel component of the wave vector, with the primary influence being exerted by the temperature distribution and corre-

sponding mobility of the particles. The presence of hot protons not only skews the velocity distribution but also stabilizes the wave speed, making it less susceptible to alterations in the parallel wave number, and possibly less dampened.

As specified earlier, we so far only focused on the Alfven wave modes allowed by this dispersion model, as it was the most accessible. However, the initial code developed aimed at highlighting all the modes.

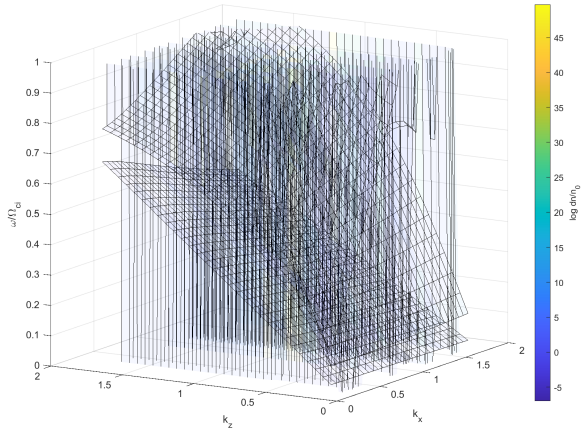

Figure 4: Dispersion relation of a cold ion plasma, and density fluctuation value

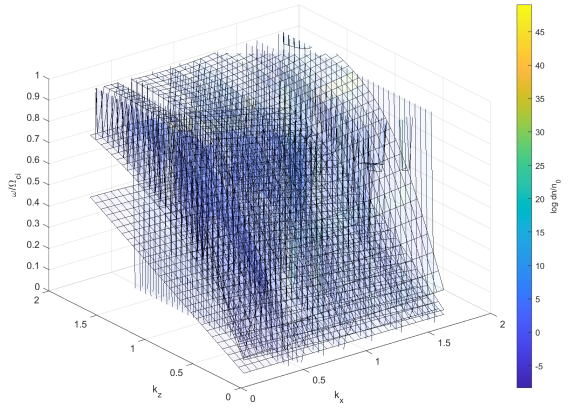

Figure 5: Dispersion relation of a dual ion temperature plasma, and density fluctuation value

As we can notice on this figures, it is hard to decipher the continuity of each modes. The solving method being only loosely dependant on the adjacent points, we can't easily isolate each continuous mode. Different methods to do so have been considered, although lack of time made it so they are still hypothetical.

5 Measurements and events

The Magnetospheric Multiscale (MMS) mission, launched by NASA in 2015, represents a landmark in space science, specifically designed to study the micro physics of magnetic reconnection, turbulence, and particle acceleration in the Earth's magnetosphere. The mission consists of four identical spacecraft flying in a tetrahedral formation, enabling high-resolution, three-dimensional measurements of the plasma environment. This unique configuration allows MMS to capture the rapid and dynamic processes occurring in Earth's magnetosphere, especially those driven by magnetic reconnection, a fundamental process that converts magnetic energy into kinetic and thermal energy in space plasmas.

In this study, we will focus on the tracking of low frequency waves, directly trackable by on field instruments. The Magnetospheric Multiscale mission utilizes different measurement techniques to capture high-resolution data on particle behavior. One of the key limitations being satellite-earth data communication, we only have access to the highest resolutions during significant events. Among these instruments is the Fly's Eye Energetic Particle Sensor (FEEPS), a system of silicon solid-state detectors designed to measure the energy of electrons. Each spacecraft is equipped with two FEEPS units, with individual detectors arranged in such a way that they provide 18 different viewing angles simultaneously. This configuration, resembling the compound eye of a fly, allows MMS to capture comprehensive, multi-directional data on energetic electron populations in space.

In addition to FEEPS, the mission is also equipped with an Energetic Ion Spectrometer (EIS), which measures both the energy and total velocity of detected ions to determine their mass. The EIS can distinguish between different ion species, such as helium and oxygen ions, particularly at higher energy levels than those detectable by the Hot Plasma Composition Analyzer (HPCA).

On October 24, 2015, the Magnetospheric Multiscale mission captured significant data while crossing the magnetopause multiple times near the dayside magnetosphere. During this period, the spacecraft observed large-scale wave events, which were accompanied by magnetic and electric field fluctuations. Notably, from 15:27:25 UT onwards, low-frequency magnetic field oscillations, peaking around 0.35 Hz, were detected. These oscillations indicate the presence of large-scale wave activity, likely related to magnetic reconnection occurring at the magnetopause. The ion velocity data recorded by MMS also revealed flows consistent with reconnection, further suggesting that these low-frequency waves were generated by this large-scale event.

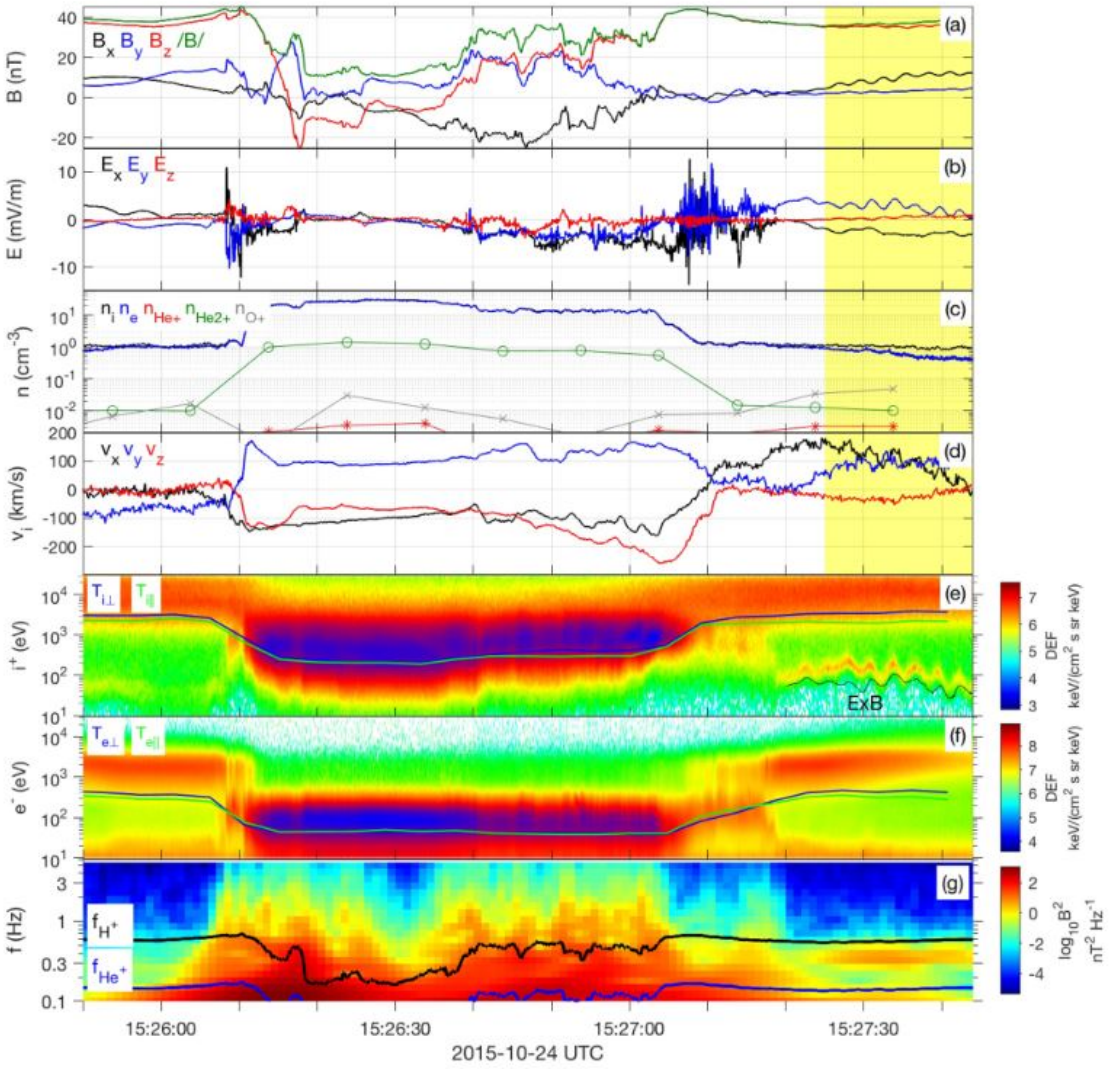

Figure 6: Measurement sequence extracted from [8], "(a) Magnetic field in GSE coordinates. (b) Electric field in GSE coordinates. (c) (black) Numberdensities of all ions from FPI, (blue) electrons from FPI, (red, green, and gray), and heavy ions (He+, He2+, and O+) from HPCA. (d) FPI ion velocity in GSE coordinates. (e) (color) FPI ion differential energy flux (DEF), (black) equivalent E × B energy for protons, (blue) perpendicular ion temperature , (green) parallel ion temperature . (f) FPI electron DEF, (blue) perpendicular electron temperature , (green) parallel electron temperature . (g) (color) Magnetic field spectrogram, (black) H + cyclotron frequency, (blue) He+ cyclotron frequency. FPI, fast plasma investigation; GSE, geocentric solar ecliptic; HPCA, hot plasma composition analyzer; MMS, magnetospheric multiscale. "

The electric field measurements during this period showed fluctuations associated with separatrix crossings, indicating interactions at the magnetospheric boundaries. Additionally, particle measurements revealed a complex plasma environment with a mixture of cold and hot ion populations. These ion populations, including protons, helium, and oxygen ions, exhibited energy fluctuations in response to the wave activity. The cold ion population, in particular, showed periodic energy changes as it interacted with the low-frequency waves. Meanwhile, electron measurements indicated density fluctuations that were more pronounced for cold protons compared to hot protons, suggesting that the cold ion population was more affected by the wave perturbations.

Using our precedent model, we can try and input the conditions of this event in our MHD wave dispersion model to estimate it's validity. The largest issue being the quantification of temperature populations, it should be pointed out that it'd be wiser to elaborate a denser routine, including an automatic binning of energy spectrum, creating hence a true j-fluid model (and not only 3 fluids) with population obtained by integration of the averaged over time spectrum. This method however is less meticulous if we take into account the necessity of global neutrality, specially at those low frequency scales.

However, we can estimate that the speed variations along the x-axis, at those, would be of 12.3 km/s on the Alfven wave, not including doppler shift. This would seem realistic according to the measurements of panel (d).

This can lead us to consider cross referencing these results on a larger scale, and have been the latest focus of this internship, although have not converged fast enough.

The model accuracy would have been measured by the error on the temperature oscillations and the speed of ions. Variations in ion temperature can lead to different resonance conditions, altering the coupling between the ions and the electromagnetic fields, and thus allow us to quickly discriminate modes. For instance, hotter ions exhibit stronger inertia, which can modify the wave-particle interaction dynamics, affecting both the amplitude and the frequency spectrum of the EMIC waves.

Similarly, the speed of ions, particularly the bulk flow velocity, is crucial for accurately modeling the phase speed and growth rate of waves. The relative motion of ions with respect to the wavefront determines the efficiency of energy transfer between the wave and the particles. Therefore, using accurate ion temperature and velocity data ensures that the model reflects the true plasma conditions, allowing for precise predictions of EMIC wave characteristics, including their spatial distribution

and temporal evolution in various magnetospheric regions. Combining this with an eploitation of the four MMS spacecraft in order to estimate the dampening, we could envision assessing other wave parameters.

6 Conclusion

The first results of our wave dispersion model appear promising, demonstrating consistency with the theoretical framework and aligning with the trends recorded in the data. These preliminary results allow that our model has successfully captured key aspects of wave-particle interactions in the plasma environment. The integration of ion temperature, velocity, and plasma physical characteristics has laid a solid foundation for further refinement. However, while these first results are encouraging, they represent only the beginning of a much larger effort needed to ensure the accuracy and robustness of the model.

Much work remains to be done to optimize the model and correlate it more accurately with experimental and observational data. Improved calibration of input parameters, such as ion distributions and magnetic field strength, is needed to achieve better alignment with real-world measurements.Further validation against diverse datasets under different magnetospheric conditions is necessary to confirm the reliability of the model in a range of scenarios. This continued effort to bridge the gap between theoretical predictions and observed phenomena will be crucial to ensure that the model can be used with confidence in practical applications, such as space weather prediction.

Moreover, phase relationships between wave components have been largely neglected in current work, despite their essential role in identifying and characterizing wave modes. Understanding phase dynamics is essential to distinguish between different wave types and to accurately model wave growth and damping processes. In the future, it will be necessary to integrate more detailed analysis of phase elements to improve the model's ability to accurately predict wave behavior. Filling this gap will not only improve the accuracy of the wave dispersion model, but also deepen our understanding of the complex interactions that govern plasma wave dynamics in space.

References

[1] Aditi Upadhyay et al. “Characteristics of ElectroMagnetic Ion Cyclotron (EMIC) waves observed at Indian Antarctic station Maitri”. In: *2019 URSI Asia-Pacific Radio Science Conference (AP-RASC)*. 2019, pp. 1–1. DOI: 10.23919/URSIAP-RASC.2019.8738455.

[2] Xingbin Tian et al. “Effects of EMIC Wave-Driven Proton Precipitation on the Ionosphere”. In: *Journal of Geophysical Research: Space Physics* 127.2 (2022). e2021JA030101 2021JA030101, e2021JA030101. DOI: https://doi.org/10.1029/2021JA030101. eprint: https://agupubs.onlinelibrary.wiley.com/doi/pdf/10.1029/2021JA030101. URL: https://agupubs.onlinelibrary.wiley.com/doi/abs/10.1029/2021JA030101.

[3] S. K. Vines et al. “EMIC Waves in the Outer Magnetosphere: Observations of an Off-Equator Source Region”. In: *Geophysical Research Letters* 46.11 (2019), pp. 5707–5716. DOI: https://doi.org/10.1029/2019GL082152. eprint: https://agupubs.onlinelibrary.wiley.com/doi/pdf/10.1029/2019GL082152. URL: https://agupubs.onlinelibrary.wiley.com/doi/abs/10.1029/2019GL082152.

[4] C.-W. Jun et al. “EMIC Wave Properties Associated With and Without Injections in The Inner Magnetosphere”. In: *Journal of Geophysical Research: Space Physics* 124.3 (2019), pp. 2029–2045. DOI: https://doi.org/10.1029/2018JA026279. eprint: https://agupubs.onlinelibrary.wiley.com/doi/pdf/10.1029/2018JA026279. URL: https://agupubs.onlinelibrary.wiley.com/doi/abs/10.1029/2018JA026279.

[5] C. F. Kennel and H. E. Petschek. “Limit on stably trapped particle fluxes”. In: *Journal of Geophysical Research (1896-1977)* 71.1 (1966), pp. 1–28. DOI: https://doi.org/10.1029/JZ071i001p00001. eprint: https://agupubs.onlinelibrary.wiley.com/doi/pdf/10.1029/JZ071i001p00001. URL: https://agupubs.onlinelibrary.wiley.com/doi/abs/10.1029/JZ071i001p00001.

[6] Khotyaintsev, Yu. V. et al. “Density fluctuations associated with turbulence and waves - First observations by Solar Orbiter”. In: *AA* 656 (2021), A19. DOI: 10.1051/0004-6361/202140936. URL: https://doi.org/10.1051/0004-6361/202140936.

[7] M. J. D. Powell. “An efficient method for finding the minimum of a function of several variables without calculating derivatives”. In: *The Computer Journal* 7.2 (Jan. 1964), pp. 155–162. ISSN: 0010-4620. DOI: 10.1093/comjnl/7.2.155.

eprint: https://academic.oup.com/comjnl/article-pdf/7/2/155/959784/070155.pdf. URL: https://doi.org/10.1093/comjnl/7.2.155.

[8] S. Toledo-Redondo et al. “Kinetic Interaction of Cold and Hot Protons With an Oblique EMIC Wave Near the Dayside Reconnecting Magnetopause”. In: *Geophysical Research Letters* 48.8 (2021). e2021GL092376 2021GL092376, e2021GL092376. DOI: https://doi.org/10.1029/2021GL092376. eprint: https://agupubs.onlinelibrary.wiley.com/doi/pdf/10.1029/2021GL092376. URL: https://agupubs.onlinelibrary.wiley.com/doi/abs/10.1029/2021GL092376.